Mantle plumes, convection and decompression melting

A. Manglik and U. R. Christensen*

National Geophysical Research Institute, Uppal Road, Hyderabad 500 007, India
*Universität Göttingen, Herzberger Landstr.180, 37075, Göttingen, Germany

Mantle plumes, narrow upwellings of hot rock, owe their origin to the instabilities of the thermal boundary layer either at 670 km depth or at the base of the mantle. These upwellings bring deep mantle material to the base of the lithosphere and are manifested on the earth's surface by positive geoid, bathymetry/topography, heat flow anomalies, and extensive volcanism. The volcanism over a mantle plume occurs due to the partial melting of hot upwelling mantle as a result of decompression. The extent of partial melting depends on the convective velocities which are obtained through a fluid dynamical modelling approach. The partial melting introduces two important effects; the latent heat effect during melting cools the plume, thus reducing the degree of melting, and the melt removal reduces the density of the mantle residue thereby introducing convective instabilities in the system. The effect of these factors on the mantle dynamics and melting rate has been studied. The results indicate formation of a swell root of depleted residue above the plume at the base of lithosphere and reduction in the melt production rate with time-varying fluctuations.

THE uppermost rigid portion of the Earth, the lithosphere, is made up of a number of plates which interact with each other forming spreading, subduction, and transform boundaries. The tectonic activity and volcanism are confined mainly to these plate margins. However, volcanism also occurs in the interior of a plate remote from any boundary, e.g. Hawaiian volcanism in the Pacific plate[1]. The geochemical signatures of this volcanism are significantly different from those of mid-oceanic ridge basalts (MORB)[2]. These centers of intraplate volcanism are called hotspots and are associated with positive geoid, topography, and heat flow anomalies. As an example, the Cape Verde hotspot on the African plate is associated with 7.6 m geoid, 1900 m bathymetry, and 16 mW m^{-2} heat flow anomaly[3]. Wilson[4] related this volcanism to elevated temperature at the base of the lithosphere. Morgan[1] proposed that the hotspots are the surface expressions of hot narrow upwellings in the Earth's mantle which convectively bring deep mantle material to the base of lithosphere. He called these mantle upwellings mantle plumes. Ever since extensive research has been carried out in this field to understand the origin of mantle plumes, mantle dynamics, physical properties of the mantle, and volume and composition of melts produced by plume melting[5,6]. In the absence of direct evidence for these narrow (≈ 150 km diameter) mantle plumes, most of the work has been restricted to numerical and laboratory experiments, whose results have been compared with constraints from geophysical observations of geoid, topography, heat flow anomalies; magmatic underplating; geochemical signatures like major and rare earth elements concentration; and geochronological data on the dates and timing of volcanism. Recently, some success has been achieved in the detection of mantle plumes in upper mantle through seismic tomography[7,8].

A mantle plume is assumed to initiate as an instability in hot thermal boundary layer that grows to form large spherical blob (Figure 1). Once the blob becomes destabilized, it starts moving upward due to its thermal buoyancy. A narrow conduit connects the plume blob with the thermal boundary layer and supplies material to the blob. This type of plume initiation model was supported by laboratory experiments on glucose syrup[9] in which a low viscosity syrup at 80°C was injected at the base of the model tank filled with relatively high viscosity glucose syrup at 20°C. The most probable location of the thermal boundary layer is the core-mantle boundary region where temperature contrast of over 1000°C exists between the lower mantle and the outer core[10]. The lateral heterogeneity in a 200–300 km thick layer above the core-mantle boundary[11,12], labelled D'', also supports this region as a probable source region of mantle plumes. However, the phase boundary between the upper and the lower mantle at 670 km depth perhaps inhibits subduction of lithospheric slabs into the lower mantle[13], resulting in ponding of subducted material at this boundary and in two-layered convection. The region around 670 km depth has also been proposed to represent a thermal boundary layer from which mantle plumes can originate. The geochemical signatures of volcanic rocks at hotspots support a model of two-layer convection, in which plumes from 670 km depth entrain some material from the lower mantle.

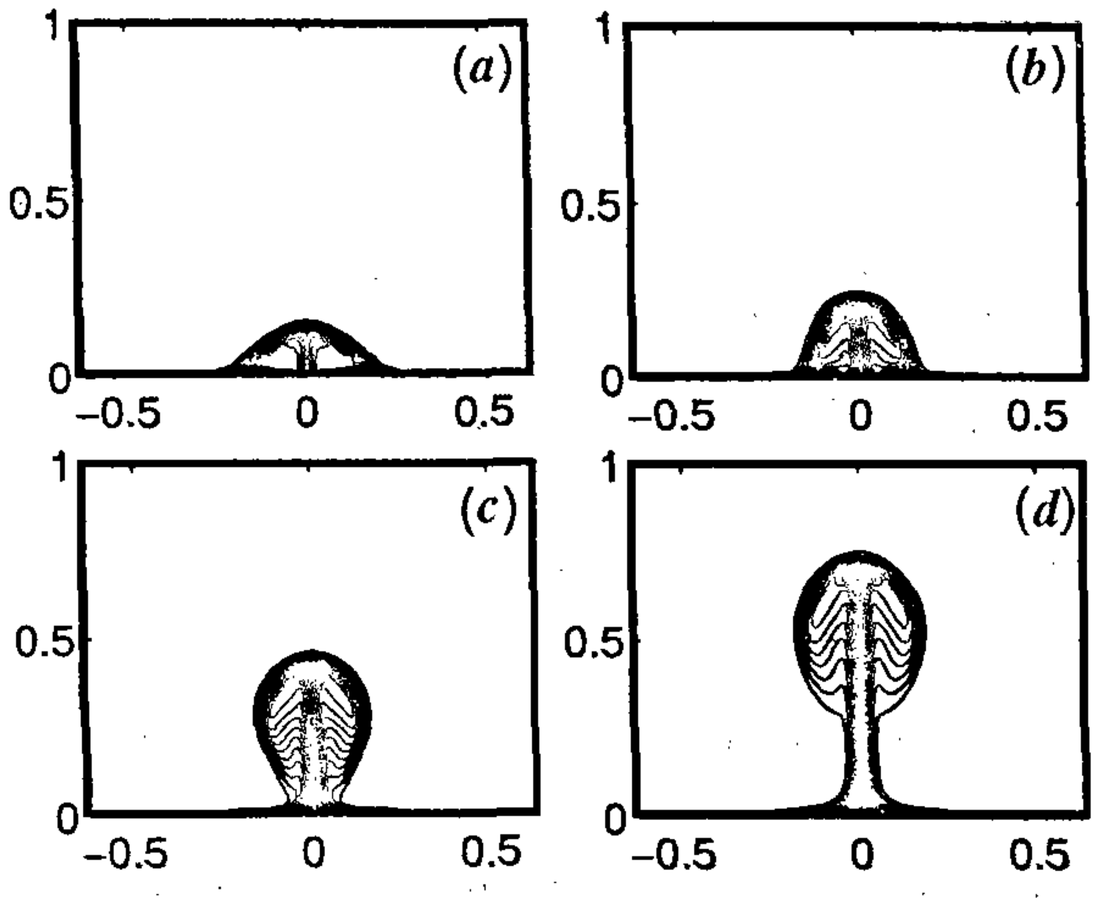

Figure 1. Results of a numerical computation to show initiation and subsequent evolution of a thermal plume in an axisymmetric cylinder for a highly temperature-dependent viscosity fluid heated from below. Frames *a–d* show the thermal structure at different times.

The convective motions in the mantle induced by plumes have been analysed by employing numerical techniques in two-dimensional, three-dimensional, cylindrical, and spherical geometries. Starting from simple models of convection of a uniform viscosity fluid in a closed box heated from below[14] to explain observed geoid and topography anomalies at hotspots, later models have grown in complexity and include highly temperature- and pressure-dependent viscosity, internal heating, plate motions, and melting in time-dependent convection. These experiments have been performed at the Rayleigh numbers representative of the earth's mantle for both the two-layered and the whole mantle convection. Two very important mechanisms that have been considered in numerical studies of mantle dynamics are the role of the endothermic phase transition at 670 km depth, and the decompression plume melting. The 670 km depth phase transition opposes the flow of material across it, favouring a tendency towards layered convection in the mantle. Christensen and Yuen[15,16] showed through numerical experiments on whole mantle convection with a phase transition that the tendency to layering increases with increasing Rayleigh number and the negativity of the Clapeyron slope. Recently, numerical results[6] have shown that the mantle may episodically alternate between two-layered and single-layer convection. The transition from two-layered to single-layer convection in these models is marked by an avalanche of new plumes. Seismological observations at some subduction zones, where the slab penetrates through the phase boundary[17] whereas it seems to remain in the upper mantle in other regions[18] and episodes of enhanced global volcanic activity during the geological past[19] have been taken as evidence for such a hybrid behaviour of mantle convection.

Melting at plumes provides another important constraint on their dynamics. The volume and composition of these melts help in constraining the depth and temperature of the melting zone. The volume of melt is estimated from the exposed volcanic rocks and the igneous rocks underplated at the Moho which are mapped by crustal seismic studies. The melt produced at plumes ascends to the Moho level. It, thereafter, gets trapped due to its relatively high density and only about one fourth of fractionated melt erupts on the surface as volcanics. White[20] estimated melt production rates at hotspots based on this estimation and found that melt production rate varies from 0.24 km^3/yr at Iceland to as low as 0.03 km^3/yr at Cape Verde hotspot. McKenzie and Bickle[21] parameterized the experimental results on melting of garnet peridotite to get solidus and liquidus temperatures and then estimated the melt production during the decompression melting of upwelling mantle at different adiabatic temperatures. White and McKenzie[22] correlated flood volcanism to the melting of a large blob of a starting mantle plume and suggested plume temperatures of 200–300°C higher than the normal mantle. Numerical codes have been developed to incorporate the effect of melting on the mantle dynamics.

During the melting of an ascending plume, the buoyancy of the material changes due to the removal of melt from the matrix and due to the latent heat effect. The melt removal reduces the density of the residue, giving rise to an upward buoyancy which is termed mantle depletion buoyancy. The latent heat effect reduces the temperature of the residue upon melting, giving a negative buoyancy component. These buoyancy effects alter the flow of plume material at the base of the lithosphere. These effects have been mainly analysed in the models of spreading ridges to explain the narrowness of the zone of crustal production[23–25]. In plume–lithosphere interaction models, Watson and McKenzie[26] and Farnetani and Richards[27] studied the effect of latent heat on the plume flow and melt production. Recently, Phipps Morgan *et al.*[28] have discussed a one-dimensional model of the Hawaiian swell root formation including the effect of mantle depletion buoyancy. Dupeyrat *et al.*[29] studied the depletion buoyancy effect in a two-dimensional isoviscous model. We have carried out work to analyse the effect of latent heat and mantle depletion buoyancy on the rate of melting and plume flow in the asthenosphere taking pressure- and temperature-dependent viscosity[30]. These results are summarized in this article. We first briefly describe the equations relevant for the fluid dynamical modelling and then discuss the steps involved in the calculation of the melt

production rate. The inferences derived from the modelling study are summarized at the end.

Fluid dynamical modelling

The convective circulation in the mantle induced by plumes is modelled by using a fluid dynamical modelling approach as used in the studies related to engineering applications. An important difference is that the mantle convects in solid state, meaning that the mantle behaves as a fluid in geological times but is solid on short time scales. However, melting of mantle is possible. An important consequence is that for the Earth's mantle the Prandtl number is of order 10^{26}, which simplifies the general Navier–Stoke's equation by allowing to ignore the inertial terms. Under the assumption of incompressible convection of a Boussinesq fluid, the momentum and incompressibility conditions are given by[31]

$$\nabla \cdot p = \nabla : \tau + \rho\, \mathbf{g}, \tag{1}$$

$$\nabla \cdot \mathbf{u} = 0, \tag{2}$$

respectively, where $\mathbf{u}$ is the velocity vector, τ is the deviatoric stress tensor, p is the pressure, and $\mathbf{g}$ is the gravity acceleration.

In the momentum equation (eq. 1), the stress tensor τ is related to the strain rate tensor $\dot{\varepsilon}$ through the constitutive rheological law[31]

$$\tau_{ij} = 2\eta(p, T, C, \dot{\varepsilon})\dot{\varepsilon}_{ij}, \tag{3}$$

and the strain rate is related to the velocity by

$$\dot{\varepsilon}_{ij} = \frac{1}{2}(\partial_i u_j + \partial_j u_i). \tag{4}$$

In plume-induced mantle convection, the circulation is mainly driven by the thermal buoyancy. Therefore, one needs to solve the energy equation

$$\rho C_p \partial_t T + \mathbf{u} \cdot \nabla T = \nabla \cdot (k \nabla T) + Q, \tag{5}$$

where T is the temperature, C_p is the specific heat, k is the thermal conductivity, and Q is the rate of volumetric heat generation.

The thermal and mantle depletion buoyancy contributions are included by computing the density variation from

$$\rho = \rho_0 [1 + \alpha(T_0 - T) - \beta D], \tag{6}$$

where ρ_0 and T_0 are the reference density and reference temperature, respectively, β is the chemical buoyancy coefficient[32] and D is the degree of depletion.

Melt generation

McKenzie and Bickle[21] synthesized the experimenta results on melting of garnet peridotite and obtained a parameterized form of the solidus and liquidus curves for mantle rocks as

$$P = (T_s - 1100)/136 + 4.968 \times 10^{-4} \exp(1.2 \times 10^{-2}(T_s - 1100)), \tag{7}$$

$$T_l = 1736.2 + 4.343\, P + 180 \tan^{-1}(P/2.2169) \tag{8}$$

for quantification of melt production (Figure 2). In the above equations, P is the pressure in GPa, T_s is the solidus temperature, and T_l is the liquidus temperature They also obtained an empirical relation between the melt fraction and temperature which is given as

$$X - 0.5 = T^* + [(T^*)^2 - 0.25](0.4256 + 2.988T^*), \tag{9}$$

where X is the melt fraction and T^* is given by

$$T^* = \frac{T - 273 - (T_s + T_l)/2}{T_l - T_s}.$$

During the melting process, some amount of heat is absorbed due to the latent heat effect reducing the

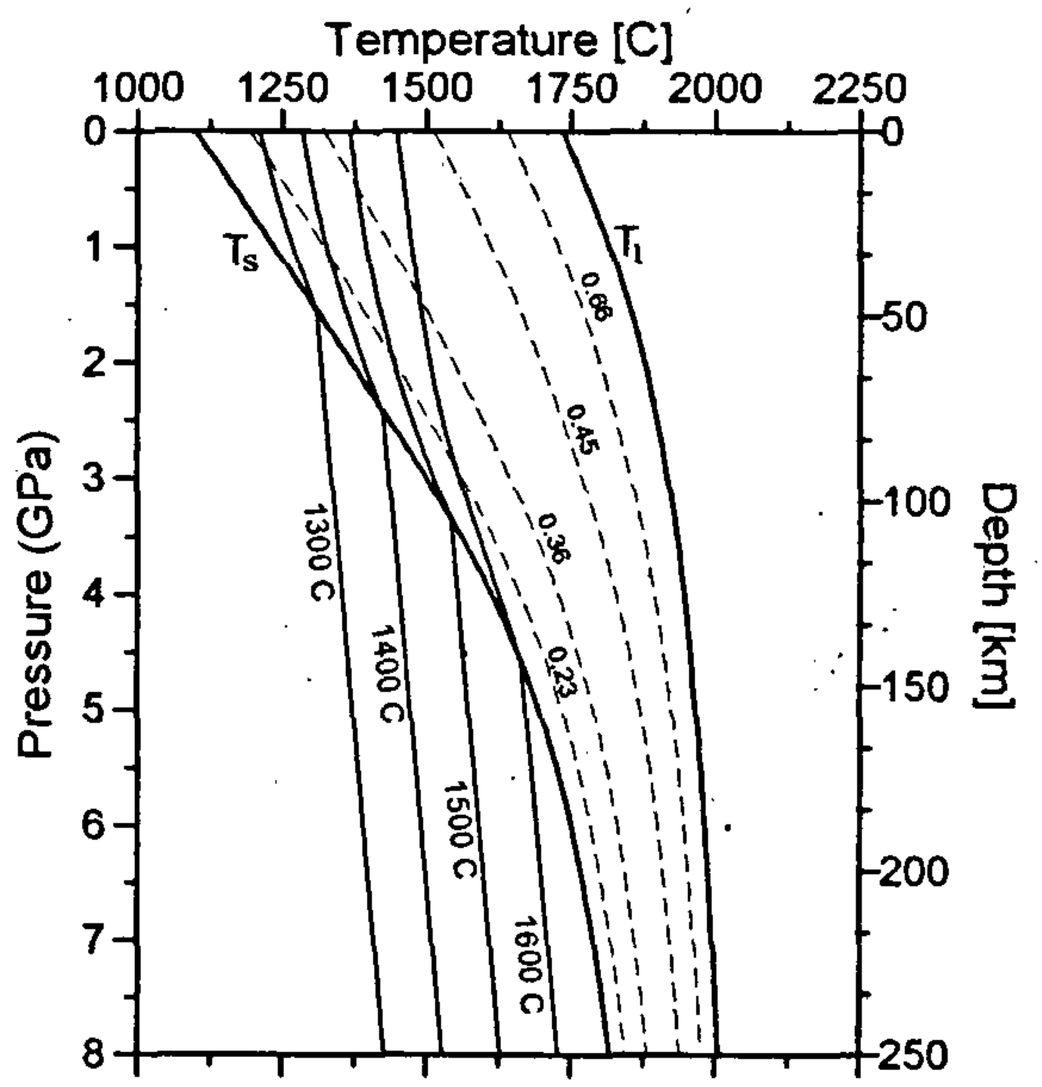

Figure 2. Melt production rate curves after McKenzie and Bickle[21] but for the entropy change of 400 J/kg K. T_s and T_l are the solidus and liquidus curves for garnet peridotite and the dashed curves are the isolines of constant melt fraction. The lines marked by different temperature values, e.g. 1300°C are the adiabatic temperatures which become curved during melting due to the latent heat effect.

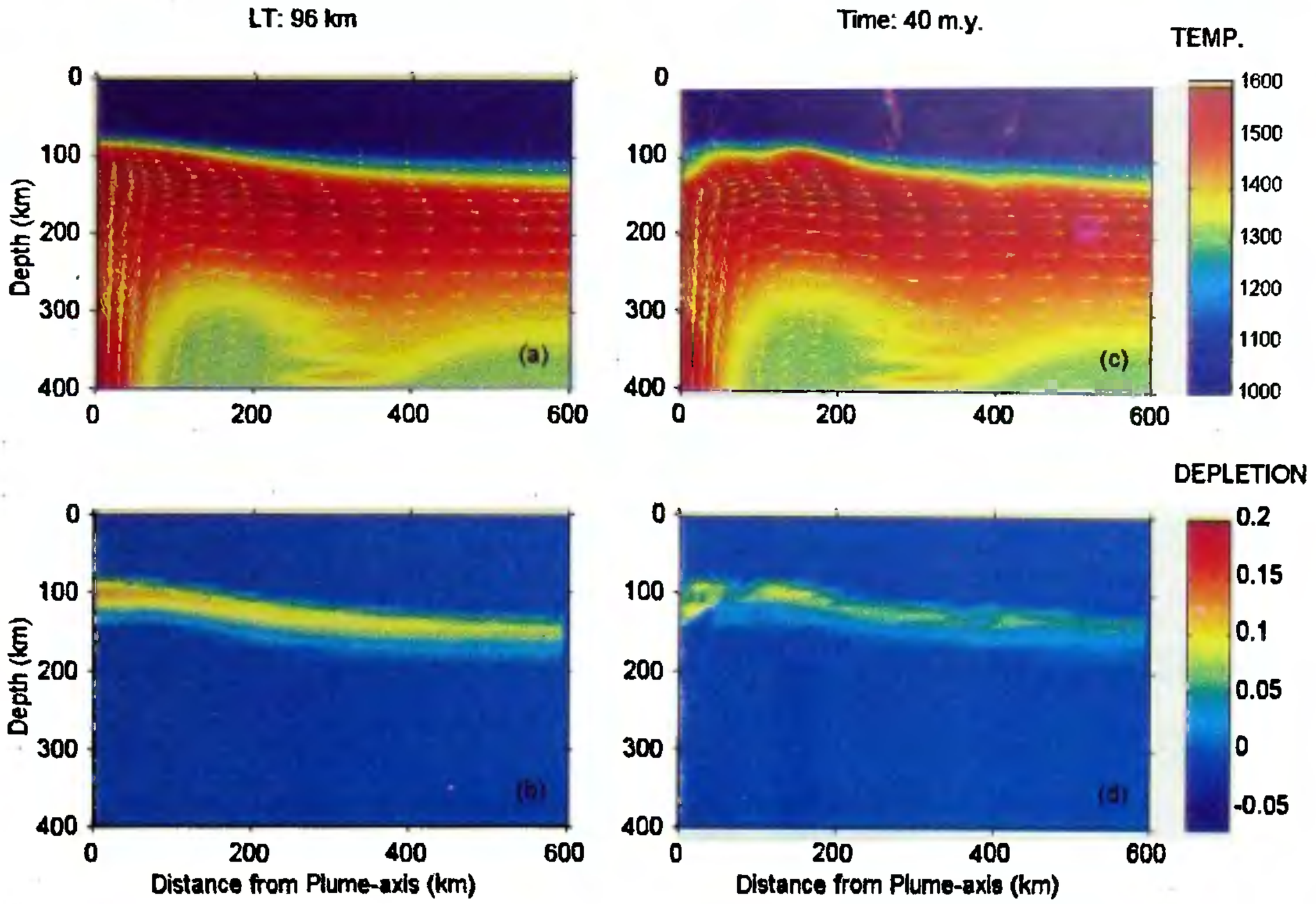

Figure 3. Plume convection under a 96 km thick lithosphere at 40 m.y. time. The results are: *a*, temperature and flow beneath the lithosphere; *b*, degree of depletion of mantle residue in the absence of chemical buoyancy effect; *c*, temperature and flow, and *d*, degree of depletion for the same case including the effect of chemical buoyancy.

temperature of the medium and hence the melt production. This effect is not included in eq. (9). McKenzie[33] applied this correction in melting calculations under the assumption of constant entropy of melting. Since a direct implementation of such latent heat-corrected melting calculation is computationally tedious, Watson and McKenzie[26] suggested a parameterized form of the latent heat correction for use in melting calculations in mantle convection codes. We computed our results using the above parameterization, but with a value of 400 J/kg K for the entropy change during melting instead of 250 J/kg K as used by Watson and McKenzie[26] in their original calculations. We computed melting using a Lagrangian tracer particle method[31].

Results

We studied the effect of mantle depletion buoyancy on the melting and mantle dynamics using a two-dimensional spline-based finite element program. The main results of our computations are summarized here. In our computations the viscosity was highly pressure- and temperature-dependent. The results were computed for different cases of lithospheric thicknesses but only the results for the case of thick lithosphere of 96 km are presented here. Figure 3 shows the temperature, flow, and melt fraction at 40 m.y. time without (*a*, *b*) and with (*c*, *d*) the effect of depletion buoyancy. The results indicate the formation of a thick root at the base of the lithosphere in presence of depletion buoyancy effect. The flow in presence of depletion buoyancy has small-scale instabilities sinking from the base of the lithosphere to the asthenosphere.

The evolution of the rate of melt production with time for lithospheric thicknesses of 60 and 96 km, respectively, is shown in Figure 4. The results for the case of no depletion buoyancy are shown by the solid lines and those with the chemical buoyancy are shown by dashed lines. The melt production rate is significantly high for melting under thin lithosphere. In this case, melt production is initially high but gradually decreases when no chemical buoyancy is included. Inclusion of chemical buoyancy effect, however,

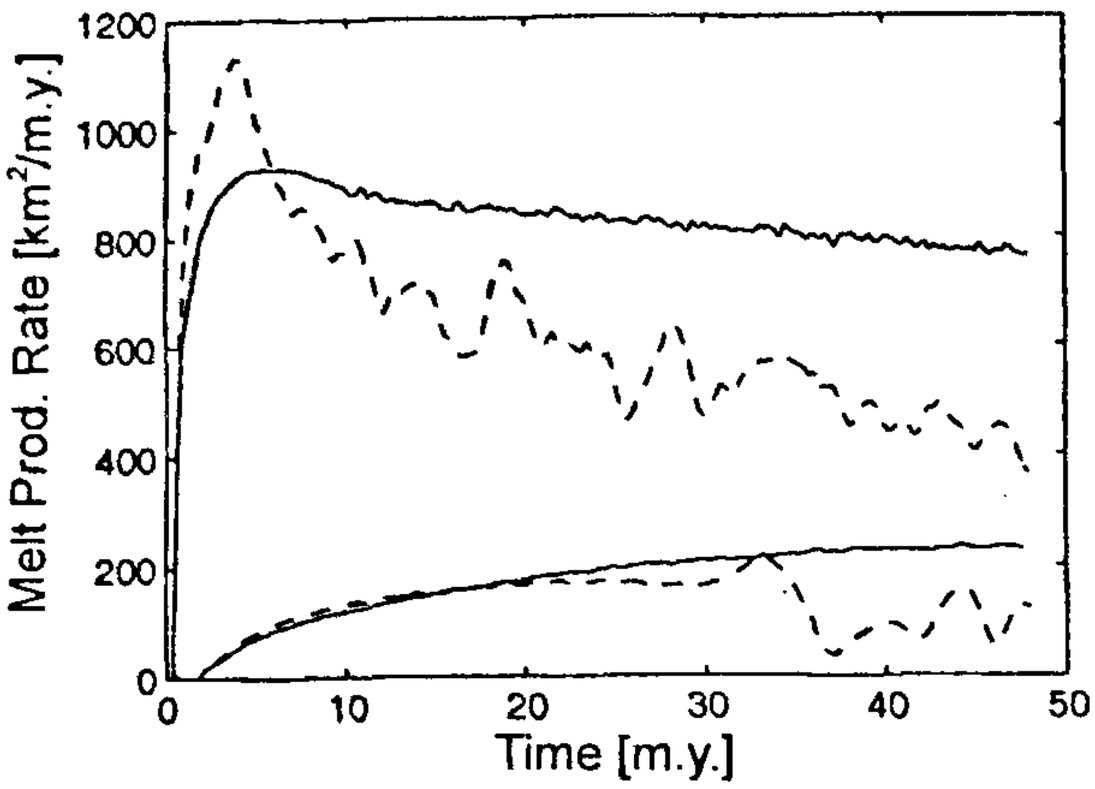

Figure 4. Evolution of melting rate for plume flow beneath thin (60 km) and thick (96 km) lithospheres. The results with and without the effect of chemical buoyancy are shown by dashed and solid curves, respectively (after Manglik and Christensen[30]).

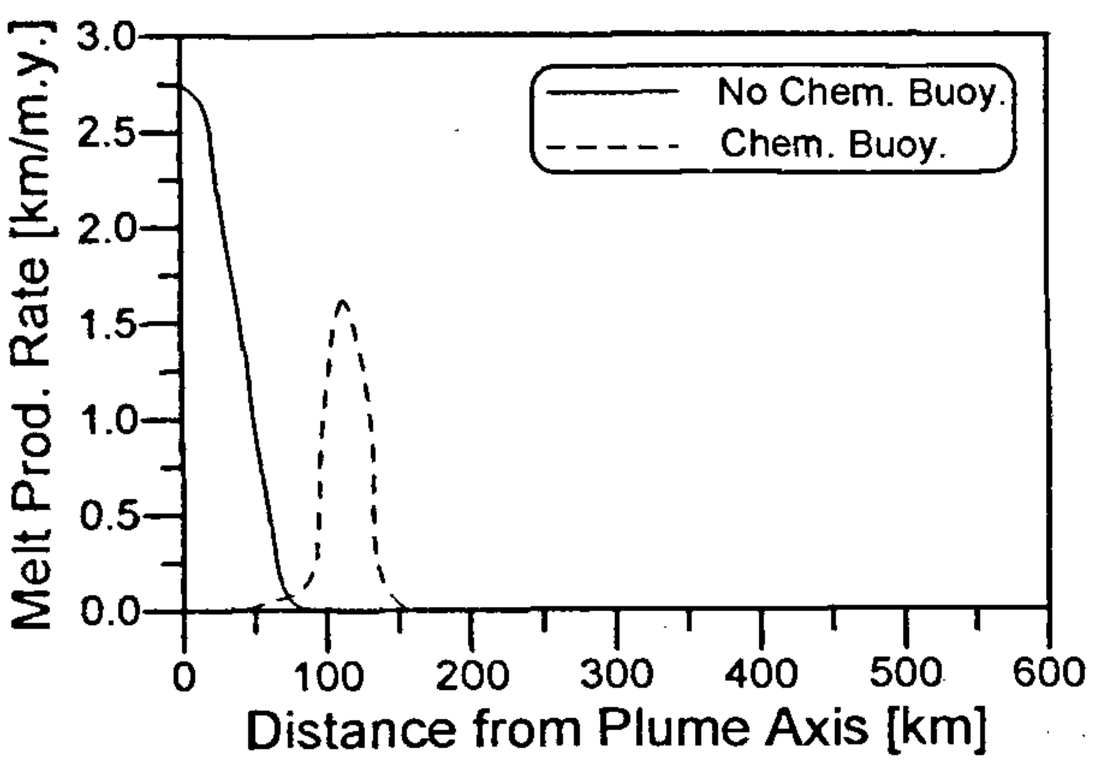

Figure 5. Depth integrated melt production rate as a function of distance from the plume-axis at 40 m.y. time for melting under 96 km thick lithosphere to show a lateral shift with time in the zone of maximum melt production due to the formation of swell root (after Manglik and Christensen[30]).

enhances melting rate at initial times and significantly reduces melting at later times. For thick lithosphere case, in the absence of chemical buoyancy the melt production rate increases steadily with time and is smooth. In the presence of depletion buoyancy effect, the melt production rate decreases by 50%. This reduction in the melting rate is the result of accumulation and gravitational trapping of the depleted residue below the thinned lithosphere above the plume that inhibits further plume upwelling to shallow depth in the zone of melting. Also, the melt production rate significantly fluctuates with time in presence of depletion buoyancy. Another effect of the presence of the depleted residue at the plume axis is the lateral shift in the zone of maximum melt production. This result for 96 km thick lithosphere case is shown in Figure 5. The results were obtained by vertically integrating the melt production in different columns in lateral direction. The results show a lateral shift in the zone of maximum melt production with time.

Conclusion

These results can be summarized to state that the mantle depletion buoyancy effect significantly influences the flow of plume material by introducing small-scale instabilities in the asthenosphere and by forming a depleted swell root at the plume center inhibiting further upwelling. This results in the reduction in the melt production and a lateral shift in the volcanism.

Although the numerical modelling of mantle convection with plumes has grown in complexity, there are still many unresolved issues, e.g. how to introduce plate boundaries in the modelling and how the continents influence the asthenospheric flow pattern. In the Indian context, the Deccan volcanism is one of the best examples of plume–lithosphere interaction. The three-dimensional studies of interaction of a starting plume with moving continental lithosphere undergoing stretching can be taken up in the future in order to understand the mantle dynamics and the tectonics of the western part of the Indian continent.

1. Morgan, W. J., *Nature*, 1971, **230**, 42–43.
2. Hofmann, A. W., *Nature*, 1997, **385**, 219–228.
3. Courtney, R. C. and White, R. S., *Geophys. J. R. Astron. Soc.*, 1986, **87**, 815–868.
4. Wilson, J. T., *Can. J. Phys.*, 1963, **41**, 863–870.
5. White, R. S. and McKenzie, D., *J. Geophys. Res.*, 1995, **100**, 17543–17585.
6. Tackley, P. J., *Rev. Geophys.*, 1995, 275–282.
7. Nataf, H. C. and VanDecar, J., *Nature*, 1993, **364**, 115–120.
8. Wolfe, C. J., Bjarnason, I. Th., VanDecar, J. C. and Solomon, S. C., *Nature*, 1997, **385**, 245–247.
9. Griffith, R. W. and Campbell, I. H., *Earth Planet. Sci. Lett.*, 1990, **99**, 66–78.
10. Boehler, R., *Nature*, 1993, **363**, 534–536.
11. Nataf, H.-C. and Houard, S., *Geophys. Res. Lett.*, 1993, **20**, 2371–2374.
12. Loper, D. E. and Lay, T., *J. Geophys. Res.*, 1995, **100**, 6397–6420.
13. Schubert, G., Yuen, D. A. and Turcotte, D. L., *Geophys. J. R. Astron. Soc.*, 1975, **42**, 705–735.
14. McKenzie, D., Roberts, J. M. and Weiss, N. O., *J. Fluid Mech.*, 1974, **62**, 465–538.
15. Christensen, U. R. and Yuen, D. A., *J. Geophys. Res.*, 1984, **89**, 4389–4402.
16. Christensen, U. R. and Yuen, D. A., *J. Geophys. Res.*, 1985, **90**, 10291–10300.
17. Fischer, K. M., Creager, K. C. and Jordan, T. H., *J. Geophys. Res.*, 1991, **96**, 14403–14427.
18. Fukao, Y., Obayashi, M., Inoue, H. and Nenbau, M., *J. Geophys. Res.*, 1992, **97**, 4809–4822.

19. Stein, M. and Hofmann, A. W., *Nature*, 1994, **372**, 63–68.
20. White, R. S., *Philos. Trans. R. Soc. London*, 1993, **A342**, 137–153.
21. McKenzie, D. and Bickle, M. J., *J. Petrol.*, 1988, **29**, 625–679.
22. White, R. S. and McKenzie, D., *J. Geophys. Res.*, 1989, **94**, 7685–7729.
23. Sotin, C. and Parmentier, E. M., *Geophys. Res. Lett.*, 1989, **16**, 835–838.
24. Scott, D. R. and Stevenson, D., *J. Geophys. Res.*, 1989, **94**, 2973–2988.
25. Jha, K., Parmentier, E. M. and Morgan, J. P., *Earth Planet. Sci. Lett.*, 1994, **125**, 221–234.
26. Watson, S. and McKenzie, D., *J. Petrol.*, 1991, **32**, 501–537.
27. Farnetani, C. G. and Richards, M. A., *J. Geophys. Res.*, 1994, **99**, 13813–13833.
28. Phipps Morgan, J., Morgan W. J. and Price, E., *J. Geophys. Res.*, 1995, **100**, 8045–8062.
29. Dupeyrat, L., Sotin, C. and Parmentier, E. M., *J. Geophys. Res.*, 1995, **100**, 497–520.
30. Manglik, A. and Christensen, U. R., *J. Geophys. Res.*, 1997, **102**, 5019–5028.
31. Christensen, U. R., *J. Geophys. Res.*, 1992, **97**, 2015–2036.
32. Su, W. and Buck, R., *J. Geophys. Res.*, 1993, **98**, 12191–12205.
33. McKenzie, D., *J. Petrol.*, 1984, **25**, 713–765.

ACKNOWLEDGEMENTS. A.M. is thankful to CSIR and Deutscher Akademischer Austauschdienst, Germany for the support under exchange programme. A.M. is also thankful to Dr R. N. Singh and Dr Harsh K. Gupta for their encouragement.

RESEARCH ARTICLES

The systematics of fundamental particles and unstable nuclear systems using the concept of continuity and discreteness

Raja Ramanna and Anju Sharma

National Institute of Advanced Studies, Indian Institute of Science Campus, Bangalore 560 012, India

In this review, a new method is proposed based on Cantor's Theory of Cardinality to analyse the experimental data on unstable nuclear systems which includes fundamental particles and their flavours, β-decay including spin and parity, α-decay and the systematics of the energy levels of light nuclei. The method also derives a formula for the binding energies of unstable nuclei. All this is based on the theory of discreteness and continuity.

THE earliest review on nuclear physics was written nearly sixty years ago by H. A. Bethe and his associates[1] to explain various nuclear phenomena within the framework of quantum theory. The review which was published in a series of three articles incorporated a thorough and comprehensive study of the developments in the field of nuclear physics at that time. The review covered almost every aspect of the nucleus ranging from α-, β-, γ-radioactivity, nuclear reactions, nuclear forces and many-body effects, etc.

Bethe's work was epoch-making and influenced all other research subsequent to his paper. For many years it was considered that the nuclear forces obtained by various experiments were sufficient to understand all nuclear phenomena but unfortunately the strong many-body nature of the problem shifted the fundamental approach to the study of nuclear models and has been the approach of all later workers. Though enormous developments have taken place in nuclear sciences, such as the discovery of magic numbers, excited states of nuclei up to high energies, discovery of parity, to mention only a few that fall in this category, an overall picture of nuclear systems which includes fundamental particles is still incomplete and will probably remain as such.

Even though there has been a continuous progress in dealing with nuclear systems and fundamental particles, there still is a lack of a coherent formulation which would permit an analysis of all observed phenomena in a fundamental way. In place of a single unifying theory, there are scattered islands of knowledge in a sea of seemingly uncorrelated observations. So far, attempts have been made to formulate several theories and models to understand various physical phenomena, which concentrate only on small sections of the observed behaviour. Experiments are often performed, guided by existing theories to mainly confirm certain features predicted by them, rather than making